α_1-Adrenergic Receptors Regulate Neurogenesis and Gliogenesis

Manveen K. Gupta, Robert S. Papay, Chris W. D. Jurgens, Robert J. Gaivin, Ting Shi, Van A. Doze, and Dianne M. Perez

Department of Molecular Cardiology, NB50, the Lerner Research Institute, the Cleveland Clinic Foundation, Cleveland, Ohio (M.K.G., R.S.P., R.J.G., T.S., D.M.P.); and Department of Pharmacology, Physiology, & Therapeutics, University of North Dakota, School of Medicine & Health Sciences, Grand Forks, North Dakota (C.W.D.J., V.A.D.)

ABSTRACT

The understanding of the function of α_1-adrenergic receptors in the brain has been limited due to a lack of specific ligands and antibodies. We circumvented this problem by using transgenic mice engineered to overexpress either wild-type receptor tagged with enhanced green fluorescent protein or constitutively active mutant α_1-adrenergic receptor subtypes in tissues in which they are normally expressed. We identified intriguing α_{1A}-adrenergic receptor subtype-expressing cells with a migratory morphology in the adult subventricular zone that coexpressed markers of neural stem cell and/or progenitors. Incorporation of 5-bromo-2-deoxyuridine in vivo increased in neurogenic areas in adult α_{1A}-adrenergic receptor transgenic mice or normal mice given the α_{1A}-adrenergic receptor-selective agonist, cirazoline. Neonatal neurospheres isolated from normal mice expressed a mixture of α_1-adrenergic receptor subtypes, and stimulation of these receptors resulted in increased expression of the α_{1B}-adrenergic receptor subtype, proneural basic helix-loop-helix transcription factors, and the differentiation and migration of neuronal progenitors for catecholaminergic neurons and interneurons. α_1-Adrenergic receptor stimulation increased the apoptosis of astrocytes and regulated survival of neonatal neurons through phosphatidyl-inositol 3-kinase signaling. However, in adult normal neurospheres, α_1-adrenergic receptor stimulation increased the expression of glial markers at the expense of neuronal differentiation. In vivo, S100-positive glial and βIII tubulin neuronal progenitors colocalized with either α_1-adrenergic receptor subtype in the olfactory bulb. Our results indicate that α_1-adrenergic receptors can regulate both neurogenesis and gliogenesis that may be developmentally dependent. Our findings may lead to new therapies to treat neurodegenerative diseases.

It is now recognized that neurogenesis continues in the mammalian brain after birth. The areas of the most active neurogenesis are the subventricular zone (SVZ) of the lateral ventricles and the subgranular zone (SGZ) of the hippocampus (Lie et al., 2004). The SVZ contains neural stem cells (NSCs) whose progenitors migrate through defined pathways, such as the rostral migratory stream (RMS) that directs neuroblasts to the olfactory bulb where they mature into interneurons. In the hippocampus, new neurons are born in the SGZ and become functioning granule cells (Santarelli et al., 2003). The prevailing view is that NSCs are glial fibrillary acidic protein (GFAP)-positive cells of a radial glial lineage (Morshead and van der Kooy, 2004). NSCs are self-renewing and multipotent cells that generate neurons, astro-

ABBREVIATIONS: SVZ, subventricular zone; AR, adrenergic receptor; bHLH, basic helix-loop-helix; BrdU, 5-bromo-2′-deoxyuridine; CAM, constitutively active mutant; EGF, epidermal growth factor; EGFP, enhanced green fluorescence protein; FBS, fetal bovine serum; FGF, fibroblast growth factor; NSC, neural stem cell; PBS, phosphate-buffered saline; RMS, rostral migratory stream; RT, room temperature; SGZ, subgranular zone; TAP, transient amplifying progenitor; TUNEL, terminal deoxynucleotidyl transferase; VEGF, vascular endothelial growth factor; GFAP, glial fibrillary acidic protein; KO, knockout; DMEM, Dulbecco's modified Eagle's medium; FACS, fluorescence-activated cell sorting; NMDA, N-methyl-D-aspartate; PKC, protein kinase C; PCR, polymerase chain reaction; MAP2, microtubule-associated protein-2; D-PBS, Dulbecco's phosphate-buffered saline; PD98059, 2′-amino-3′-methoxyflavone; SB203580, 4-(4-fluorophenyl)-2-(4-methylsulfinylphenyl)-5-(4-pyridyl)1H-imidazole; SP600125, anthra[1–9-cd]pyrazol-6(2H)-one; LY294002, 2-(4-morpholinyl)-8-phenyl-1(4H)-benzopyran-4-one hydrochloride; Go6983, 3-[1-[3-(dimethylamino)propyl]-5-methoxy-1H-indol-3-yl]- 4-(1H-indol-3-yl)-1H-pyrrole-2,5-dione; ICI-118,551, ($\pm$)-1-[2,3-(dihydro-7-methyl-1H-inden-4-yl)oxy]-3-[(1-methylethyl)amino]-2-butanol.

cytes, and oligodendrocytes (Lie et al., 2004). Under normal conditions, neurogenesis in other central nervous system (CNS) regions is minimal, suggesting that specific mechanisms regulate where new neurons are produced.

The α_1-adrenergic receptor (AR) subtypes (α_{1A}, α_{1B}, and α_{1D})[1] are G-protein-coupled receptors that regulate the sympathetic nervous system by binding and transducing the signals of norepinephrine and epinephrine. Within the peripheral nervous system, α_1-AR activation is known to regulate the cardiovascular and other organ systems. Within the CNS, it has proven more difficult to ascribe α_1-AR functions, let alone the subtype to a particular function, because of poorly selective ligands and weak antibodies (Jensen et al., 2009). However, evidence links central α_1-ARs to the regulation of plasticity (Sirviö and MacDonald, 1999) and stimulation of GABAergic interneurons (Papay et al., 2006). Studies have also indirectly suggested a potential role of α_1-ARs in neurogenesis. α_1-AR activation increases vascular endothelial growth factor (VEGF) mRNA (Gonzalez-Cabrera et al., 2003), and VEGF has been suggested to increase the proliferation of neuronal precursors (Jin et al., 2002). VEGF localizes to the choroid plexus (Maharaj et al., 2006), which receives strong adrenergic innervation to regulate its secretory functions (Lindvall and Owman, 1981). The α_1-ARs stimulate the shedding of epidermal growth factor (EGF) and fibroblast growth factor (FGF) (Chen et al., 2006), factors needed to maintain NSC niches. [^{3}H]Prazosin binding sites are found in SVZ neuroepithelia in rat embryonic day-13 embryos (Pabbathi et al., 1997) and in adult mice engineered to overexpress α_{1A}-ARs tagged with enhanced green fluorescent protein (EGFP) to localize the receptor (Papay et al., 2006). Using α_1-AR promoters expressing EGFP tags with or without the receptor (Papay et al., 2004, 2006), we identified a cell type in the SVZ in vivo that coexpressed markers of NSCs and/or their progenitors that can be labeled by 5-bromo-2-deoxyuridine (BrdU). Subsequent studies on isolated neonatal neurospheres derived from normal mice and mice engineered to overexpress constitutively activate mutant (CAM) receptors or with their α_1-ARs knocked out (KO) revealed that α_1-ARs play an important role in the regulation of NSC/progenitors and their differentiation into neurons. In contrast, α_1-ARs expressed on adult neurospheres and isolated from normal mice regulated gliogenesis. However, α_1-ARs colocalized with both glial and neuronal progenitors in the adult mouse olfactory bulb.

Materials and Methods

Animal Use. Mice were housed and provided veterinary care in an Association for Assessment and Accreditation of Laboratory Animal Care-accredited animal care facility. The experimental protocols used in this study conform to the *Guide for the Care and Use of Laboratory Animals* published by the U.S. National Institutes of Health and was approved by the Animal Care and Use Committee at our institutions.

Immunohistochemistry. For in vivo analysis, mice were cardiac-perfused, and brain sections wee made using a vibrotome as described previously (Papay et al., 2004, 2006). Primary antibodies used were rabbit notch1 at 1:50 (Santa Cruz Biotechnology, Santa Cruz, CA), mouse nestin at 1:100, rabbit Dlx2 at 1:200 (both from Chemicon, Temecula, CA), and rabbit vimentin at 1:5000 (Abcam Inc., Cambridge, MA). For in vitro analysis, cells were fixed in 4% paraformaldehyde for 30 min. Coverslips were blocked in 6% bovine serum albumin and 0.3% Trition X-100 in PBS for 1 h at room temperature (RT) and then incubated with the primary antibody chicken microtubule-associated protein-2 (MAP2) at 1:5000 (Novus Biologicals, Inc., Littleton, CO), rabbit NG2 at 1:7000 (a gift from Bill Stallcup), or mouse GFAP at 1:3000 (Chemicon) in blocking buffer for 24 h at 4°C. The coverslips were washed three times in PBS and then incubated with the corresponding secondary antibodies donkey anti-chicken cy5 at 1:500 (Jackson Immunoresearch Laboratories Inc., West Grove, PA), goat anti-rabbit 488 at 1:4000, and goat anti-mouse 568 at 1:4000 (both from Molecular Probes, Carlsbad, CA) for 1 h at RT. Coverslips were washed three times in PBS, transferred to a microscope slide with Vectashield containing 4′, 6′-diamidino-2-phenylindole (Vector Laboratories, Burlingame, CA). Sections were analyzed using a confocal laser-scanning microscope (Aristoplan; Leica Micosystems, Inc., Deerfield, IL). Confocal images represent optical sections of 2 to 3 μm axial resolution and an average of three to six line scans. Fluorescence in red, green, blue, and purple channels were collected simultaneously. Confocal images were reassembled, and the images were presented as a projection. Colocalization was confirmed in single confocal sections in which EGFP fluorescence is present in the same cell with each cell-type marker.

Neonatal Neurosphere Isolation and Culture. Neurospheres were isolated from the periventricular regions of postnatal day 3 pups of neonatal normal, CAM α_{1A}, CAM α_{1B}, and their corresponding KO mice. Periventricular regions were digested for 20 min at 37°C in 3 ml of 0.05% trypsin, 0.53 mM EDTA, and 0.001% DNAase in D-PBS (10 mM HEPES, pH 7.6, and 0.5 g of glucose/500 ml). Six milliliters of B27 complete media (DMEM/Ham's F-12, 1× B27 (Gibco), 20 ng/ml recombinant human EGF (Stem Cell Technologies, Vancouver, BC, Canada), 10 ng/ml recombinant human FGF (Abcam), 0.0002% heparin (Sigma), and 100 U/ml penicillin/streptomycin) was added, and the sample was centrifuged at 100g for 7 min. The supernatant was removed and the pellet titrated in 5 ml of D-PBS with a 5-ml pipette for 5 min. Cells were passed through a large 70-μm cell strainer into a 50-ml conical tube and centrifuged at 100g. Cells were resuspended in D-PBS, centrifuged, and the pellet was resuspended in D-PBS. Cells were passed through a 30-μm cell strainer (CellTrics; Partec, Swedesboro, NJ), centrifuged, and resuspended into 10 ml of B27 complete media and counted. Cells were split and fed every 2 to 3 days by centrifugation and replating. After 1 to 2 weeks, we picked 20 neurospheres from the culture of dissociated tissue. Of these isolated neurospheres, approximately 60% maintained good neurosphere growth when dissociated. We finally isolated six neurospheres for cell lines, which were all positive for nestin/notch and α_1-AR expression, except for the KO cell lines. After reaching sufficient density, neurospheres were passaged by mechanical dissociation or with accutase (Sigma, St. Louis, MO). Neurospheres used for experimental purposes were all taken from third or later passages.

Radioligand Binding. Membranes were prepared from neurospheres as described previously (Zuscik et al., 1998). Saturation or competition binding was performed using the α_1-AR antagonist [^{125}I]iodo-2-[β-(4-hydroxyphenyl)-ethyl-aminomethyl]tetralone or the β-AR antagonist ^{125}I-cyanopindolol as the radioligand as described previously (Zuscik et al., 1998). Data were analyzed using Prism software (GraphPad Software Inc., San Diego, CA). Various AR antagonists used in radioligand binding were purchased from Sigma-Aldrich.

Neurosphere Assay. Neurospheres were dissociated with accutase and mechanical titration and were diluted to single-cell level for replating in individual uncoated 24-well plates. The percentage of single cells (percentage of cloning efficiency) that regenerate neurospheres was determined.

Differentiation Assay. Neurospheres were centrifuged at 100g for 7 min to remove growth factors and were resuspended in B27 media without EGF/FGF but were supplemented with 2% FBS. Cells

---

[1] After the α_{1C}-AR was reclassified as the α_{1A}-AR, the α_{1C}-AR designation is no longer used.

were then transferred to a 24-well plate containing a sterile pre-coated poly(D-lysine)/laminin coverslip (Biocoat; BD Biosciences, San Jose, CA). For phenylephrine-induced differentiation, 10 μM phenylephrine was added daily to B27 complete media in the presence of 1 μM propranolol and 0.1 μM rauwolscine to block β- and α_2-ARs, respectively. Coverslips were fixed with 4% paraformaldehyde in PBS for 30 min at RT and then washed twice with PBS for 5 min and used for immunohistochemistry or stored in PBS at 4°C. At least three different coverslips (each containing 40–300 cells) were analyzed from three separate experiments.

In Vivo BrdU Incorporation. Mice were injected intraperitoneally with BrdU at 150 mg/kg body weight. Two hours after the injection, the mice were anesthetized and cardiac-perfused, and brains were sectioned as described previously (Papay et al., 2006). In chase experiments, normal mice or mice that received bottle water containing cirazoline at 10 mg/l for 12 weeks were injected twice daily intraperitoneally with BrdU at 50 mg/kg body weight for 2 weeks, then sacrificed at 2 days, 7 days, and 14 days after the last BrdU injection. Sections were first rinsed in 0.9% NaCl and then incubated in 1 N HCl in 0.9% NaCl at 37°C for 30 min. Sections were rinsed with 0.1 M borate buffer, pH 9.0, and then rinsed with Tris-buffered saline. Sections were then incubated with mouse anti-BrdU (Chemicon) at 1:5000 in blocking buffer for 2 days at 4°C and then incubated with Alexa Fluor 568 goat anti-mouse IgG (Molecular Probes) at 1:4000 in blocking buffer for 1 h at RT. Specimens were rinsed twice with distilled water before incubation with 2 ml of 10 mM copper sulfate in 50 mM ammonium acetate for 1 h at RT to remove autofluorescence. Samples were then rinsed twice with distilled water before being returned to PBS, transferred to a microscope slide containing Vectashield with 4′, 6′-diamidino-2-phenylindole, and BrdU nuclei were counted using confocal microscopy followed by stereology.

Stereology. The optical dissector technique was used to estimate the density of BrdU$^+$ and/or Nestin$^+$ cells in the SGZ of the dentate gyrus of the hippocampus and the SVZ of the lateral ventricles. Random slices were selected, and the number of BrdU$^+$ cells and volume of each structure were computed with Stereo Investigator software (MBF Bioscience; MicroBrightField Inc., Williston, VT). Cell density was expressed in cells per cubic millimeter, and the number of BrdU- and Nestin-labeled cells per section was then averaged.

Real-Time PCR. Neurospheres were treated with phenylephrine (10 μM) or 1% FBS for 1, 3, or 7 days in the presence of rauwolscine (0.1 μM) and propranolol (1 μM). Total RNA was isolated using the RNeasy kit (QIAGEN, Valencia, CA), and 2 μg of RNA was reverse-transcribed using oligo(dT) primer with Superscript II Reverse Transcriptase (Invitrogen, Carlsbad, CA). Quantitative real-time PCR was performed with an iCycler (Bio-Rad, Hercules, CA) using iQ SYBR Green Supermix (Bio-Rad). The cDNA was amplified with primers for various neural transcriptional factors. The primers used included the following: Dlx2, 5′-aagggtgtctgtgcagatttc-3′ and 5′-cgtcgcagctttcacaact-3′; Mash-1, 5′-catctcccccaactactcca-3′ and 5′-ccagcagctcttgttcctct-3′; Math-1, 5′-acatctcccagatcccacag-3′ and 5′-gggcatttggttgtctcagt-3′; Ngn-1, 5′-gagccggctgacaatacaat-3′ and 5′-ctcaggttcttcctggagca-3′; nestin, 5′-gaggggacctggaacatgaa-3′ and 5′-gtccattctccatcctccca-3′; NeuroD, 5′-gtgatgctggtactactggaattg-3′ and 5′-gcaactgcatgggagttttc-3′; α_{1A}-AR, 5′-ggttcccaaaggaaacctgt-3′ and 5′-ggtttcataccagggtggtg-3′; α_{1B}-AR, 5′-tctcagccaagtcctggttt-3′ and 5′-gcgaacacctttacctgctc-3′; and α-tubulin, 5′-ggctgccctagagaaggatt-3′ and 5′-aaacatccctgtggaagcag-3′. Samples were analyzed for relative gene expression using the $2^{-\Delta\Delta C_T}$ method (Livak and Schmittgen, 2001) and were normalized to α-tubulin gene expression as an internal control. Data were obtained from three independent experiments performed in duplicate.

Pathway Analysis. Normal neonatal neurospheres were pretreated for 1 h with individual inhibitors (either 20 μM PD98059, 10 μM SB203580, 10 μM SP600125 (all from Calbiochem, San Diego, CA), 20 μM LY294002 (Cell Signaling Technology, Danvers, CA), or

0.5 μM Go6983 (Calbiochem) and then stimulated with phenylephrine (10 μM) for 3 days. Neurospheres were then lysed and subjected to SDS-polyacrylamide gel electrophoresis, transferred to polyvinylidene difluoride membrane, and probed with antibodies against mouse GFAP at 1:1000 or chicken MAP2 at 1:3000. Membranes were washed and incubated with horseradish peroxidase-conjugated secondary antibodies. Chemiluminescence detection was performed by incubating membranes with SuperSignal West Pico Chemiluminescent Substrate (Pierce, Rockford, IL) followed by exposure onto X-ray film.

Neuronal Cell Types. Normal neurospheres were stimulated with 10 μM phenylephrine for 0, 3, 7, or 14 days, and lysates were subjected to Western blot analysis. Nonspecific binding was blocked by incubation with 5% milk and 0.1% Tween 20 in Tris-buffered saline for 2 h at RT. The membranes were then incubated with primary antibody in blocking buffer against goat anti-GAD-65/67 (1:100), rabbit anti-β_1-integrin (1:500; Santa Cruz Biotechnology), sheep anti-tyrosine hydroxylase (1:200), rabbit anti-NMDAR1 (1:100; Chemicon), sheep anti-dopamine β-hydroxylase (1:3000; Novus Biologicals), or monoclonal anti-β-actin (Sigma) overnight at 4°C with gentle agitation. Membranes were washed three times with 0.1% Tween 20 in Tris-buffered saline and incubated with the appropriate horseradish peroxidase-coupled secondary antibodies for 1 h at RT followed by chemiluminescence detection.

Apoptosis Assay. Neurospheres were grown and analyzed for apoptosis by using the FlowTACS Apoptosis Detection Kit (Trevigen, Gaithersburg, MD). Terminal deoxynucleotidyl transferase end-labeling of the free 3′-hydroxyl residues in the fragmented DNA was performed according to manufacturer's instructions. In brief, normal neonatal neurospheres were treated with 10 μM phenylephrine for 0 (control), 2, or 3 days, fixed in 3.7% formaldehyde, permeabilized, and labeled with primary antibodies against MAP2 and GFAP and the terminal deoxynucleotidyl transferase enzyme, followed by Strep-Fluorescein treatment and appropriate secondary antibodies. Cells were also treated with propidium iodide to label necrotic cells, which were not counted. Cells were analyzed under a fluorescence microscope. Total cells counted ranged from 40 to 240 per coverslip using at least three different cell preparations.

Migration Assay. The effect of α_1-AR stimulation on progenitor cell migration was determined by Boyden chamber assay as described previously (Sun et al., 2001). In brief, neurospheres derived from normal, CAM, and KO mice were dissociated in DMEM/Ham's F-12 medium without growth factors at a density of 10^6 cells/transwell (Costar; Corning Life Sciences, Acton, MA) using a 0.4 μM membrane. Phenylephrine (10 μM) was added to the lower well, and
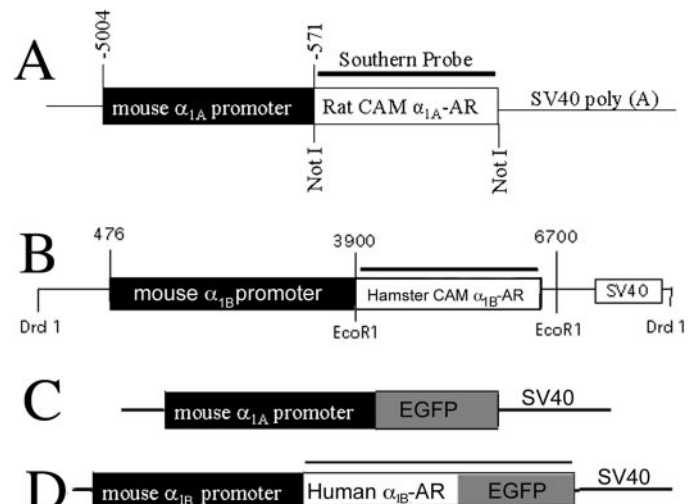

Fig. 1. Constructs used for systemic overexpression in transgenic mice. A, CAM α_{1A}-AR; B, CAM α_{1B}-AR; C, α_{1A}-AR promoter-driving EGFP only; D, α_{1B}-AR EGFP-tagged receptor.

after 48 h, the media from each of the upper and lower wells were aspirated, and cells were scraped and assayed for DNA content using the CyQuant Cell Proliferation assay kit (Invitrogen) and a Cyto-Fluor II fluorescent plate reader.

Isolation of Adult Normal Neurospheres. Adult normal neurospheres were isolated from the periventricular regions of 2 to 3 months normal mice. Periventricular regions were dissected in a Petri dish containing 10 ml of NeuroCult Tissue Collection Solution (StemCell Technologies). After dissection, the collection solution was

discarded, and the tissue was divided into two piles, minced for 1 min in 1 ml of NeuroCult Dissociation Solution, and transferred to a 15-ml sterile conical tube being careful not to introduce air bubbles. The mincing was repeated twice. The pooled minced tissue was incubated for 7 min at 37°C in a beaker of prewarmed water. The suspension was gently mixed with 3 ml of NeuroCult Inhibition Solution, avoiding air bubbles. The mixture was centrifuged at 100g for 7 min, and the supernatant was removed. The pellet was resuspended in 1 ml of NeuroCult Resuspension Solution and triturated
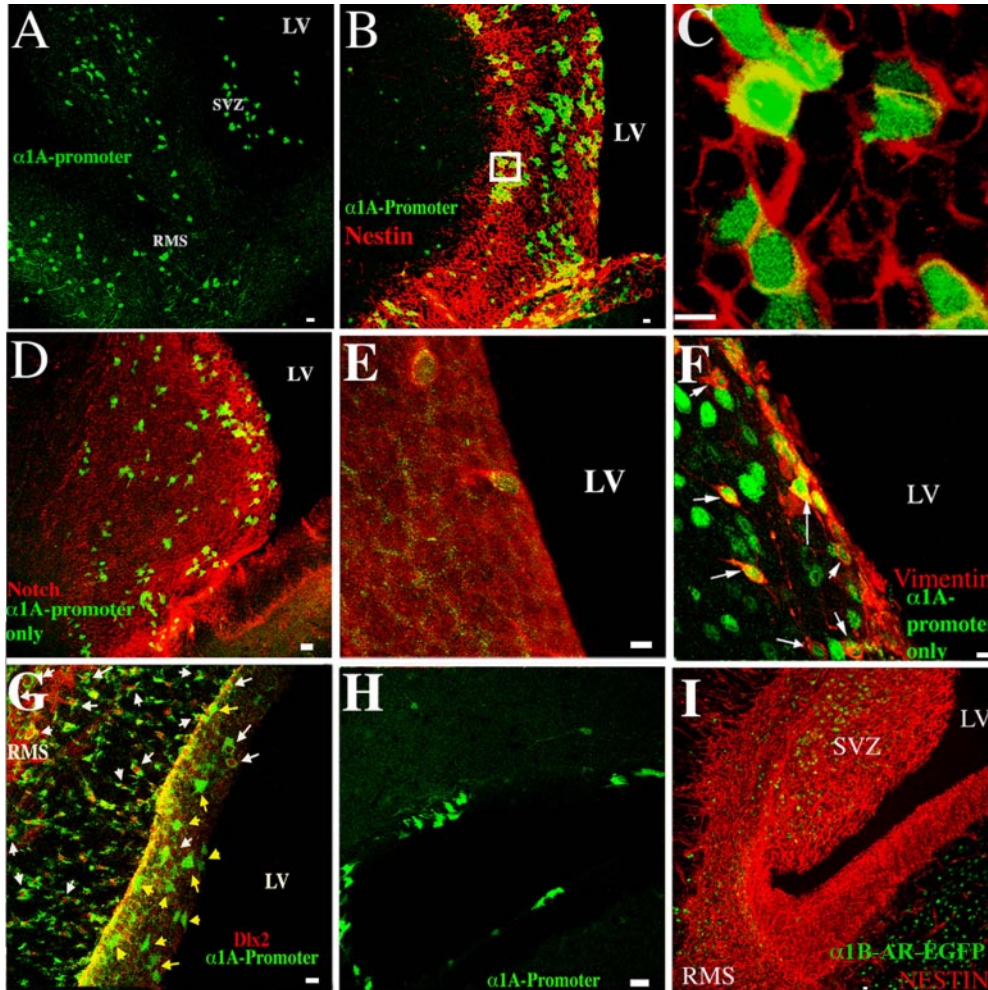
Fig. 2. α_{1A}-AR promoter-EGFP cells localize in the SVZ in vivo. A, α_{1A}-AR promoter-EGFP-expressing cells (green) are found in the SVZ and RMS of adult mice. B, α_{1A}-AR promoter-EGFP cells are abundant in the SVZ, where nestin (in red) is located. C, magnification of the boxed area in B. α_{1A}-AR promoter-EGFP cells colocalize with nestin. D, α_{1A}-AR promoter-EGFP cells are abundant in the SVZ, where Notch-1 (in red) is located. Some α_{1A}-AR promoter-EGFP cells colocalize with Notch-1 (E) or vimentin (F) near the lateral ventricle (LV) border. G, some α_{1A}-AR promoter-EGFP cells express Dlx2 in the nucleus (white arrows) in the SVZ and RMS, whereas other α_{1A}-AR promoter-EGFP cells do not (yellow arrows). H, α_{1A}-AR promoter-EGFP cells line the fourth ventricle. I, α_{1B}-AR-EGFP-tagged cells are not localized near the ependymal border. J, FACS of dissociated periventricular cells from normal mice (control) or three different α_{1A}-promoter EGFP mice (fluorescein isothiocyanate 1–3). Approximately 44.4% of periventricular cells express EGFP. Mice were aged 2 to 3 months. White bar, 10 μm.
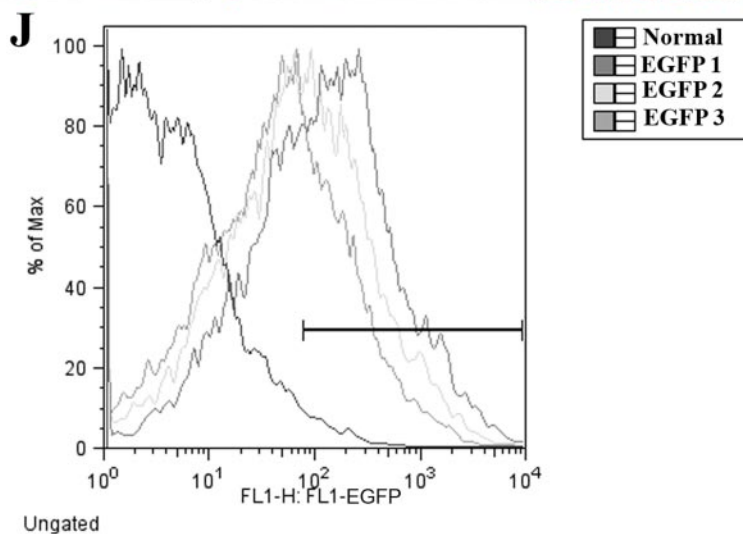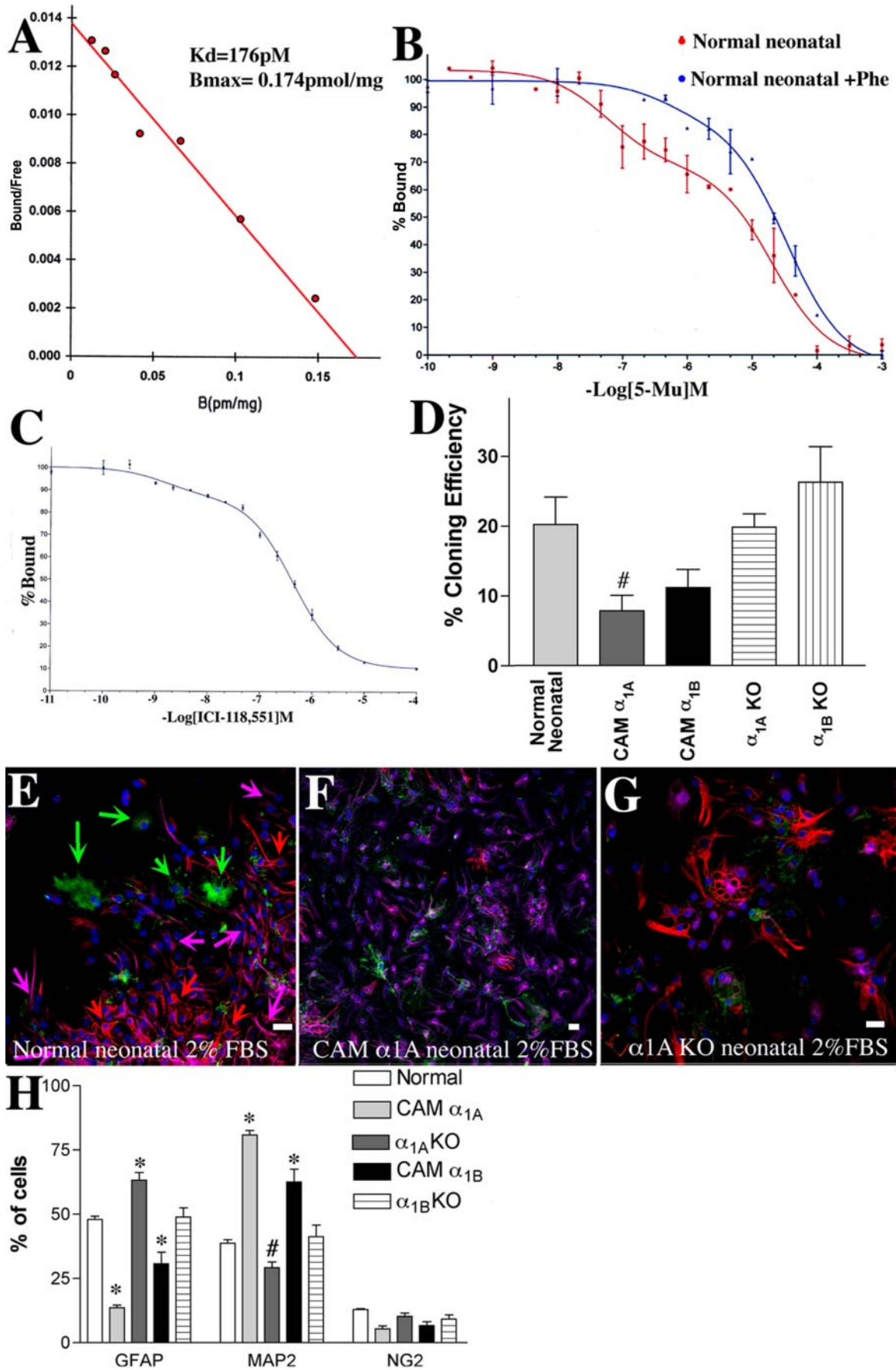
Fig. 3.

using a sterile P1000 pipette tip 15 times until a smooth and creamy suspension was achieved. NeuroCult Resuspension Solution was added to a final volume of 10 ml, and the sample was gently mixed. The cells were washed three times by centrifugation at 100g for 7 min, and the pellet was resuspended in 1 ml of NeuroCult Resuspension Solution. The pellet was first resuspended in 1 ml of B27 Adult Proliferation Media (StemCell Technologies), followed by Resuspension Solution to a total volume of 10 ml. Cells were passed through a large 70-μm cell strainer into a 50-ml conical tube, passed through two more 70-μM cell strainers, and into a sterile 15-ml polypropylene tube. A cell sample was assessed for viability with trypan blue, and the remaining cells were pipetted into two T-162 flasks, each containing 40 ml of B27 complete media. The next day, the media were collected, and the cells were centrifuged and replated into six T-162 flasks. After 1 to 2 weeks, several large neurospheres were isolated and expanded for experimental studies.

Fluorescence-Activated Cell Sorting Analysis. The SVZ regions were dissected from normal and α_{1A}-promoter-EGFP mouse brains and dissociated in 0.25% trypsin solution in DMEM. The number of EGFP$^+$ cells was determined by fluorescence-activated cell sorting (FACS).

Statistical Analysis. One-way analysis of variance followed by the Bonferroni post hoc test was used for multiple data sets. For comparisons between two data sets, a Student's paired t test was used. The data are presented as mean $\pm$ S.E.M. P values less than 0.05 were considered to be significant.

Results

Transgenic Mice. We previously created several mouse models that systemically express either the α_{1A}- or α_{1B}-AR subtypes using large fragments of the isogenic promoters isolated from mouse genomic DNA (Fig. 1). Two of our models overexpress the α_1-ARs with CAMs that cause the receptor to be activated without the need for agonists and to increase subtype-specific signaling (Fig. 1, A and B). We have previously characterized these mutations both in vitro and in vivo to verify their constitutive activity (Hwa et al., 1997; Zuscik et al., 2000). Because antibodies against α_1-ARs have poor avidity in endogenous tissues (Jensen et al., 2009), we also created α_1-AR transgenic mice with and without EGFP tags (Fig. 1, C and D). All of these mice have been characterized previously (Papay et al., 2004, 2006).

To verify promoter fidelity, the mouse α_{1A}- and α_{1B}-AR promoters used in generating the transgenic mice were expressed in α_1-AR-expressing and null cell lines (Zuscik et al., 1999; O'Connell et al., 2001) and demonstrated predicted

fidelity and regulation by transcription factors and known stimuli. Protein comparison studies were also performed using α_{1A}-promoter EGFP, α_{1A}-AR-EGFP fusion, and α_{1A}-AR KO mice in which the α_{1A}-AR locus was knocked in with the β-galactosidase gene. EGFP and β-galactosidase expression patterns throughout the brain seemed to be exact (Papay et al., 2006). Because the α_{1B}-AR KO mice were not made with the β-galactosidase knock-in, we performed additional studies to verify this subtype's promoter fidelity. We confirmed α_{1B}-AR expression in transgenic mice expressing WT and CAM receptors under the direction of the α_{1B}-AR promoter by measuring receptor levels in both positive and negative tissues and by in situ mRNA hybridization studies in the mouse brain (Zuscik et al., 2000). The promoters seem to direct expression that is similar to if not identical with the endogenous gene, although temporal studies were not investigated.

α_1-AR SVZ Localization In Vivo. In performing localization studies in the brain using adult EGFP-expressing mice, we noticed an intriguing cell type in the SVZ that expressed EGFP using the α_{1A}-AR promoter (Fig. 2A). We showed that these assumed α_{1A}-AR-expressing cells are located near the ependymal layer, the SVZ, and RMS with a migratory morphology. These SVZ cells do not express markers for any glia or neuronal cell type (S100, CC1, NG2, NeuN, βIII-tubulin). To determine whether these cells could be stem/progenitor cells, we performed immunohistochemistry in the EGFP-expressing mice using a series of NSC/progenitor markers. EGFP colocalized in the SVZ with cells that express nestin (Fig. 2, B and C), notch-1 (Fig. 2, D and E), and vimentin (Fig. 2F). The transcription factor Dlx2 is expressed in transient amplifying progenitors (TAP) and neuroblasts. Some of the EGFP cells in the SVZ expressed Dlx2, but others did not (Fig. 2G). We noticed that EGFP cells in the SVZ were of a mixed population; cells near the ependymal layer rarely expressed Dlx2 but did express other NSC markers, suggesting that they were pre-TAP cells (Fig. 2G, yellow arrows). In contrast, EGFP cells further inside the SVZ expressed Dlx2 (Fig. 2G, white arrows), but not other NSC markers, suggesting that they were TAPs or neuroblasts. These unique EGFP cells were also located in all of the ventricles, such as the fourth ventricle (Fig. 2H), but did not colocalize with stem/progenitor markers. In contrast, α_{1B}-AR-EGFP cells did not localize within the SVZ (Fig. 2I) but were observed further downstream in the migratory path. FACS analysis of EGFP cells present in the SVZ of adult α_{1A}-promoter EGFP mice suggests that approximately 44% of cells contain EGFP (Fig. 2J). However, not all of these cells may be progenitors, because the α_{1A}-AR-EGFP is also expressed on mature cell types (Papay et al., 2006). These results are consistent with the α_{1A}-AR being expressed in NSCs and/or TAP cells in vivo and regulating the neurogenic process.

Neurosphere Characterization. One way to functionally define NSC/progenitors is to isolate and culture cells so that they form neurospheres, which express mostly progenitor cells. Because we are not sure of all the types of progenitors that express the α_{1A}-AR, neurosphere analysis is probably addressing the bulk of cell responsiveness. We initially picked 20 neurospheres from each culture of dissociated tissue. Of these isolated neurospheres, approximately 60% maintained good neurosphere growth when dissociated. We finally isolated six neurospheres to establish cell lines, which were all positive for nestin/notch. To first determine whether

Fig. 3. AR expression in neonatal neurospheres and pluripotency. A, [^{125}I]Iodo-2-[β-(4-hydroxyphenyl)-ethyl-aminomethyl]tetralone saturation binding of normal neonatal neurospheres. B, competition binding with 5-methylurapidil indicates that normal neonatal neurospheres expressed 33% of the α_{1A}-AR subtype and 67% of the α_{1B}-AR (red circles). Upon incubation with 10 μM phenylephrine (Phe) for 24 h, the subtype composition became 14% of the α_{1A}-AR and 86% of the α_{1B}-AR subtype (blue circles). C, competition binding with ^{125}I-cyanopindolol and ICI-118,551, a β_2-AR selective antagonist indicates that normal neonatal neurospheres also express a majority (86%) of the low-affinity β_1-AR subtype. D, neurosphere self-renewal assay. CAM α_{1A}-AR has a lower efficiency to regenerate neurospheres than normal or KOs. E, normal neonatal neurospheres differentiate into all three cell-types (red, GFAP; magenta, MAP2; green, NG2 upon incubation with serum, 2% FBS). F, neurospheres isolated from CAM α_{1A}-AR mice differentiated into all three cell types but were mostly neurons. G, neurospheres isolated from the α_{1A}-AR KO mice were mostly astrocytes with a reduced number of neurons. H, quantitation of cell-type differentiation by 2% FBS for neurospheres isolated from all mouse models. At least three different coverslips (each containing 40–300 cells) were analyzed from three separate experiments. White bar, 10 μm. #, $P < 0.05$; *, $P < 0.01$.

α_1-ARs were expressed in neonatal neurospheres, we performed direct radioligand binding experiments. Saturation binding indicated that neonatal neurospheres expressed 174 fmol/mg protein of α_1-ARs with a K_d of 176 pM, results similar to brain tissue known to express α_1-ARs (Fig. 3A). EGFP-derived neonatal neurospheres also express α_1-ARs, as assessed by detection of EGFP (data not shown).

To reveal the α_1-AR subtype composition, we performed competition ligand binding using 5-methylurapidil, which has 100-fold higher affinity for the α_{1A}-AR than the α_{1B}-AR subtype. We know from real-time PCR that mouse neonatal neurospheres do not express the α_{1D}-AR subtype (data not shown). We found that the composition of α_1-ARs expressed in neonatal neurospheres was 33% α_{1A}-AR and 67% α_{1B}-AR (red line, Fig. 3B). Upon incubation with 10 μM phenylephrine for 24 h, which differentiates the cells, the subtype composition switched to 14% α_{1A}-AR and 86% α_{1B}-AR (blue line, Fig. 3B). Competition binding with the β-AR radiolabel ^{125}I-cyanopindolol and the β_2-AR-selective antagonist ICI-118,551 indicates that normal neonatal neurospheres also express 86% of the β_1-AR subtype (Fig. 3C).

Neonatal Neurosphere Assay. The ability to self-renew is a key trait of neurospheres that contain NSCs. Neurospheres were dissociated and diluted to a single-cell density to determine what proportion of the single cells reformed a neurosphere (i.e., percentage of NSCs contained within the neurosphere) (Fig. 3D). CAM α_{1A}-AR-derived neurospheres had a significantly lower efficiency to regenerate neurospheres than normal or α_{1A}-AR KO, consistent with the CAM α_{1A}-AR neurospheres containing more differentiated progenitors.

Serum-Induced Pluripotency. If neurospheres contain NSCs, they should be pluripotent and differentiate into all three of the major cell types (neurons, oligodendrocytes, and astrocytes) in the brain. To determine what type of progenitors were present in each neonatal neurosphere culture, we differentiated normal neurospheres with serum (2% FBS) and found all three cell-types present (Fig. 3E). Neurospheres isolated from CAM α_{1A}-AR mice (Fig. 3F) differentiated into all three cell-types but were mostly neurons. Neurospheres isolated from the α_{1A}-AR KO mice (Fig. 3G) had greater numbers of astrocytes but reduced levels of neurons. Quantization of serum-differentiated cell types for neurospheres isolated from all mouse models is shown in Fig. 3H. CAM α_{1B}-AR neurospheres also differentiated into significantly more neurons and fewer astrocytes than normal but were not as robust as the CAM α_{1A}-AR, as evident in the lack of response in the neurospheres from the α_{1B}-AR KO.

Progenitor Proliferation. Effects of α_1-AR stimulation on proliferation rates were then confirmed using in vivo BrdU incorporation. NSCs are considered a relatively quiescent cell, whereas TAP and progenitor cells are actively dividing (Morshead et al., 1994), which are more likely to incorporate BrdU within a 2-h period. We found that the number of cells that incorporated BrdU in the adult CAM α_{1A}-AR mice increased in the SVZ of the lateral ventricle and SGZ of the hippocampus (Fig. 4, A and B), compared with normal, CAM α_{1B}-AR, or either KO. We confirmed that BrdU-positive cells were coexpressed with cells containing the α_{1A}-AR by EGFP expression, in vivo (Fig. 4C).

α_1**-AR-Induced Progenitor Differentiation.** To determine direct effects of α_1-AR stimulation on the ability to

induce differentiation, normal neonatal neurospheres (basal, Fig. 4, D and I) were incubated with phenylephrine (10 μM). Phenylephrine induced differentiation of all three cell types (Fig. 4, E and I) but under prolonged stimulation (20 days) only neurons and NG2 oligodendrocytes survived (Fig. 4, F and I). Under basal conditions, CAM α_{1A}-AR-derived neurospheres were composed mostly of MAP2-positive neuroblasts with few GFAP-positive astrocytes (Fig. 4, G and I). KO of the α_{1A}-AR increased GFAP expression but reduced MAP2 expression (Fig. 4, H and I).

α_{1A}**-AR-Induced Stem Cell Proliferation.** Because CAM α_{1A} mice have increased BrdU incorporation in fast-dividing progenitor cells, we determined whether stimulation of α_1-ARs increases proliferation of NSCs in normal mice. We found increased BrdU incorporation in normal mice
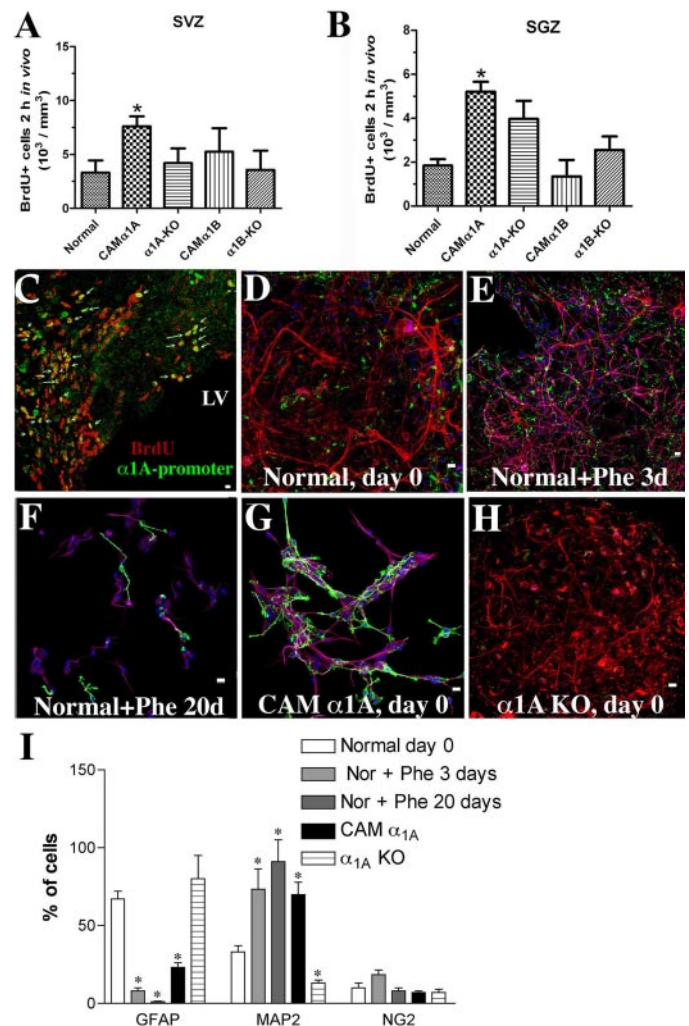

Fig. 4. α_{1A}-AR induces progenitor proliferation and differentiation. A, in vivo BrdU incorporation for 2 h indicates that 2 to 3 months CAM α_{1A}-AR mice have increased the number of proliferating progenitor cells in the SVZ (A) and SGZ (B) compared with CAM α_{1B}-AR or either KO mice. C, α_{1A}-promoter EGFP cells in the SVZ express BrdU (arrows). Normal neonatal neurospheres and phenylephrine stimulation for 0 (D, control), 3 (E), or 20 days (F) differentiates into neurons (Map2 in magenta), astrocytes (GFAP in red), and oligodendrocyte progenitors (NG2 in green). G, CAM α_{1A}-AR neurospheres at 0 days basally expressed more neurons than normal controls. KO of the α_{1A} –AR increased expression of astrocytes (H, red). I, quantified cell types for D to H. At least three different coverslips (each containing 40–300 cells) were analyzed from three separate experiments. White bar, 10 μm. $*$, $P < 0.05$.

treated with the α_{1A}-AR-selective agonist, cirazoline. Furthermore, approximately 25 to 50% of the BrdU$^+$ cells were nestin$^+$ in the normal and α_{1A}-AR-stimulated mice. Although both BrdU and nestin staining was slightly diminished after 7 and 14 days of chase, BrdU incorporation remained significantly higher at all days of chase in the cirazoline-treated mice (Fig. 5).

Regulation of Proneural Transcription Factor RNA. To determine how α_1-ARs regulate neonatal neurogenesis, we performed real-time PCR from each neonatal neurosphere line and targeted key bHLH transcription factor genes in-
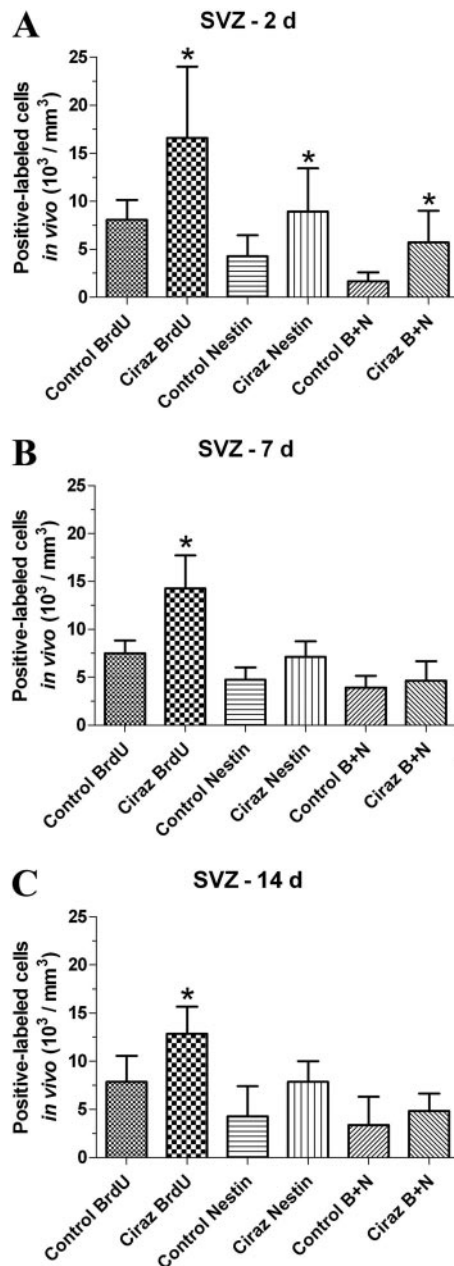
Fig. 5. α_{1A}-AR agonist increases BrdU incorporation in vivo. In vivo BrdU incorporation for 2 weeks was followed by 2 (A), 7 (B), or 14 days (C) of chase in normal mice (control) or mice that were treated with the α_{1A}-AR selective agonist, cirazoline (Ciraz), for 3 months. A, α_{1A}-AR stimulation increases the number of nestin and/or BrdU$^+$ cells at 2 days of chase. At 7 (B) and 14 days (C), α_{1A}-AR stimulation increased BrdU+ cells compared with control. ∗, $P < 0.05$ compared with matched control. B + N, BrdU$^+$/Nestin$^+$-colabeled cells.

volved in regulating neuronal differentiation (Ross et al., 2003). Relative -fold values greater than 1 indicate an increased in mRNA expression, whereas -fold values less than 1 indicate decreased mRNA expression. We differentiated using 1 instead of 2% serum to lengthen the time to complete differentiation. When differentiated by 1% serum as a control, normal neonatal neurospheres significantly increased the RNA of the α_{1B}-AR subtype, Dlx2, Mash1, Math1, Ngn1, and NeuroD, consistent with neuronal differentiation (Fig. 6, gray triangles). When stimulated by phenylephrine, CAM α_{1A}-AR neurospheres increased their own α_{1A}-AR RNA and that of the Dlx2, Mash1, and NeuroD (Fig. 6, green circles), whereas CAM α_{1B}-AR neurospheres increased the RNA of Math1 and Ngn1 (Fig. 6, red circles). Although all other genes decreased their mRNA levels in the phenylephrine-stimulated α_{1A}-AR KO, nestin RNA was the only gene to increase its mRNA levels (Fig. 6, magenta triangles), suggesting that neurosphere progenitors were more undifferentiated. The RNA of notch-1, zic-1, and sox-2 were not changed in neurospheres derived from the CAMs or KOs, suggesting that these factors are not regulated by α_1-ARs.

α_1-ARs Regulate Specific Neural Cell Types. To determine which neuronal cell types are being differentiated, we found that 10 μM phenylephrine stimulated normal neonatal neurospheres to have increased protein expression of tyrosine hydroxylase, dopamine β-hydroxylase, and GAD-65/67, markers for catecholaminergic neurons and interneurons. α_{1A}-AR KO neonatal neurospheres displayed decreased levels of each of the same cell type markers (Fig. 7A). α_1-AR stimulation also decreased the expression of β_1-integrin. However, the presence of the R1 subunit of the NMDA receptor was not expressed even though the antibody detected its presence in a whole normal brain extract.

α_1-AR Regulation of Differentiation through PI3K. To determine which signaling pathways were regulating α_1-AR-mediated neuronal differentiation, we used a battery of PKC, PI3K, and mitogen-activated protein kinase inhibitors and assessed the appearance of the postmitotic neuronal marker MAP2 in normal neonatal neurospheres. After 2 days of stimulation, 10 μM phenylephrine increased the expression of MAP2 (Fig. 7B), which decreased upon coincubation with the PI3K inhibitor LY294002 (20 μM). The PKC inhibitor Go6983 or the mitogen-activated protein kinase kinase, p38, or c-Jun NH$_2$-terminal kinase inhibitors PD98059, SB203580, and SP600125, respectively, did not decrease phenylephrine-induced MAP2 expression. Furthermore, the reciprocal loss of GFAP protein expression induced by phenylephrine was blocked using LY294002 (Fig. 7C).

α_1-ARs Induce Apoptosis of Astrocytes. Because MAP2 expression increases but GFAP expression decreases upon α_1-AR stimulation, we assessed the ability of α_1-ARs to induce apoptosis of astrocytes. Phenylephrine can increase the number of TUNEL-positive nuclei in normal neonatal neurospheres after 2 to 3 days of stimulation (Fig. 8A). However, the percentage of GFAP-expressing astrocytes with TUNEL-positive nuclei was significantly greater than TUNEL-positive cells expressing MAP2 (Fig. 8B).

α_1-ARs Regulate Neonatal Neuronal Progenitor Migration. Because α_1-ARs were expressed in vivo in cells with a migratory morphology (Fig. 2A), we explored whether α_1-ARs can affect migration of neural progenitors using in vitro transwell assays. We found that normal neurospheres stim-

ulated with phenylephrine or unstimulated CAM α_{1A}-AR-derived neurospheres increased the migration of progenitors similar to 2% serum controls (Fig. 8C), whereas α_{1A}-AR KO-derived progenitors displayed decreased migration.

α_1-ARs Regulate Adult Gliogenesis. To determine whether the effects of α_1-AR regulation of neonatal neurogenesis extended to adult mice, we performed Western analysis on adult (2–3 months) neurospheres isolated from the periventricular region of normal mice. We confirmed that two different lines of adult normal mouse neurospheres contained the stem cell markers nestin, notch 1, and vimentin but decreased their expression with α_1-AR stimulation, consistent with the role of α_1-ARs in regulating differentiation. Interestingly, adult neurospheres did not contain or alter the neuronal markers that were present in neonatal neuro-

spheres (tyrosine hydroxylase, dopamine β-hydroxylase, and GAD-65/67) but expressed and increased the glial markers CC1 and GFAP upon α_1-AR stimulation (Fig. 9A). However, adult neurospheres did contain the NR1 neuronal marker, but its expression decreased with α_1-AR stimulation. We confirmed in adult EGFP mice in vivo that either α_1-AR subtype was expressed in glial progenitors (S100-positive cells) and neuronal progenitors (βIII tubulin) in the olfactory bulb (Fig. 9, B–E).

Discussion

Although α_1-ARs are abundant in the CNS, there is limited information about neural function and subtype signaling because of the lack of highly selective ligands and avid antibod-
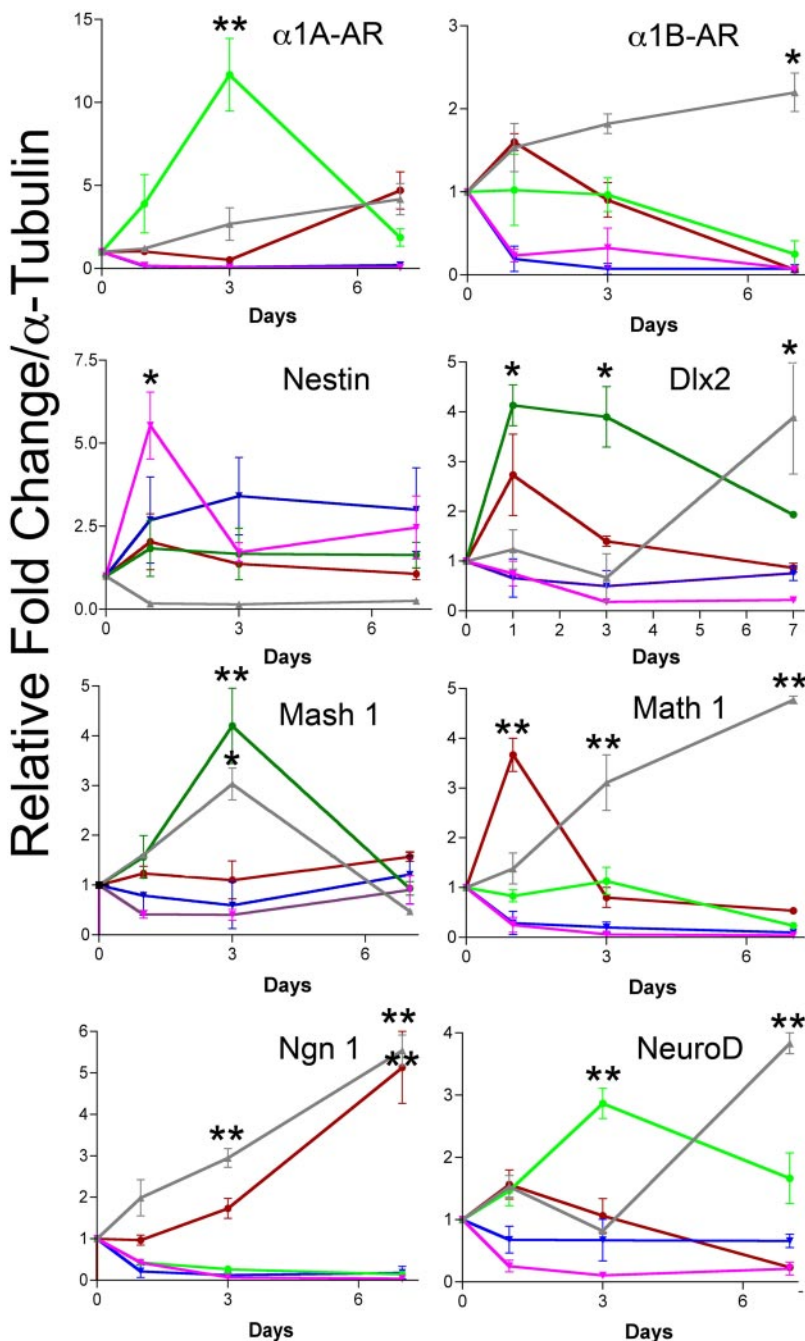
Fig. 6. α_1-ARs regulate key transcription factor mRNA involved in neonatal neuronal differentiation. RNA was isolated from neurospheres and subjected to real-time PCR. When differentiated by 1% serum, normal neonatal neurospheres significantly increased the RNA of the α_{1B}-AR subtype, Dlx2, Mash1, Math1, Ngn1, and NeuroD, consistent with neuronal differentiation (gray triangles). When phenylephrine-stimulated, CAM α_{1A}-AR neurospheres increased the RNA of Dlx2, Mash1, and NeuroD (green circles), whereas CAM α_{1B}-AR neurospheres increased the RNA of Math-1 and Ngn-1 (red circles). KO of the α_{1A}-AR subtype increased the RNA of nestin (magenta triangles), suggesting a reversion to a more undifferentiated state. Other factors tested (Notch-1, Zic-1, Sox-2) were not regulated by α_1-ARs. α_{1B}-AR KO (blue triangles). Samples are obtained from three independent experiments, performed in duplicate, and were normalized to α-tubulin gene expression as internal controls. *, $P < 0.05$; **, $P < 0.001$.

ies. Using unique and systemically expressing mouse models and KOs that circumvent these limitations, we report that α_1-AR subtypes are involved in neurogenesis and gliogenesis that may be developmentally dependent. Immunohistochemistry using stem cell markers (Fig. 2) suggest the presence of α_{1A}-ARs on stem cells and/or early progenitors.

The use of neurospheres as an in vitro model of NSCs has limitations. Whereas a single NSC in vitro is able to generate a neurosphere, in addition to NSCs, neurospheres contain neuronal and glial progenitors in different states of differen-

tiation. Therefore, neurospheres become very heterogeneous and exhibit intraclonal neural cell-lineage diversity (Suslov et al., 2002).

Regulation of the ability to regenerate neonatal neurospheres from single cells in vitro (Fig. 3D) provides evidence for the presence of α_{1A}-ARs on stem cell/early progenitors in neonatal mice. However, α_1-ARs regulate the differentiation of neurons in the neonate while switching to astrocyte and oligodendrocyte differentiation in adult mice. Further studies may indicate exactly the time in development during which the switching of cell type differentiation occurs.

In the neonate, α_1-ARs stimulated the migration and differentiation of neurosphere progenitors into catecholaminergic neurons and interneurons (Fig. 7). Neuronal differentiation was dependent on a PI3K-sensitive pathway that protects neurons from apoptosis (Figs. 7 and 8). α_1-ARs reg-
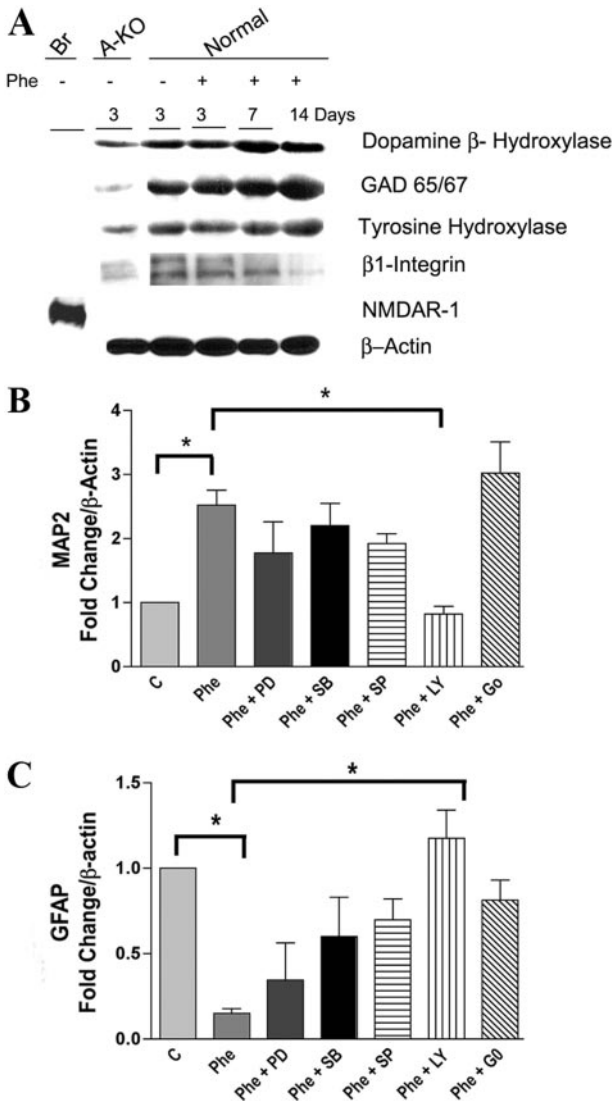

Fig. 7. α_1-ARs differentiate interneurons and catecholaminergic neurons through PI3K in neonatal neurospheres. A, Western blot analysis of normal neonatal neurospheres stimulated with phenylephrine (Phe 10 μM) increased whereas α_{1A}-AR KO decreased the expression of tyrosine hydroxylase, GAD-65/67, and dopamine β-hydroxylase. β_1-Integrin decreases expression with phenylephrine stimulation, whereas no R1 subunit of the NMDA receptor could be detected. Br, brain extract control. B, neuronal differentiation as assessed by MAP2 expression levels via Western analysis is stimulated by phenylephrine but decreased when coincubated with the PI3K inhibitor LY294002 (20 μM). C, decreased astrocyte expression as assessed by GFAP Western analysis was reduced with phenylephrine but increased when coincubated with LY294002. Other inhibitors used were 10 μM PD98059 (mitogen-activated protein kinase kinase inhibitor, PD), 10 μM SB203580 (p38 inhibitor, SB), 10 μM SP600125 (c-Jun NH$_2$-terminal kinase inhibitor, SP), and 0.5 μM Go6983 (PKC inhibitor, Go). *, $P < 0.05$; **, $P < 0.01$.
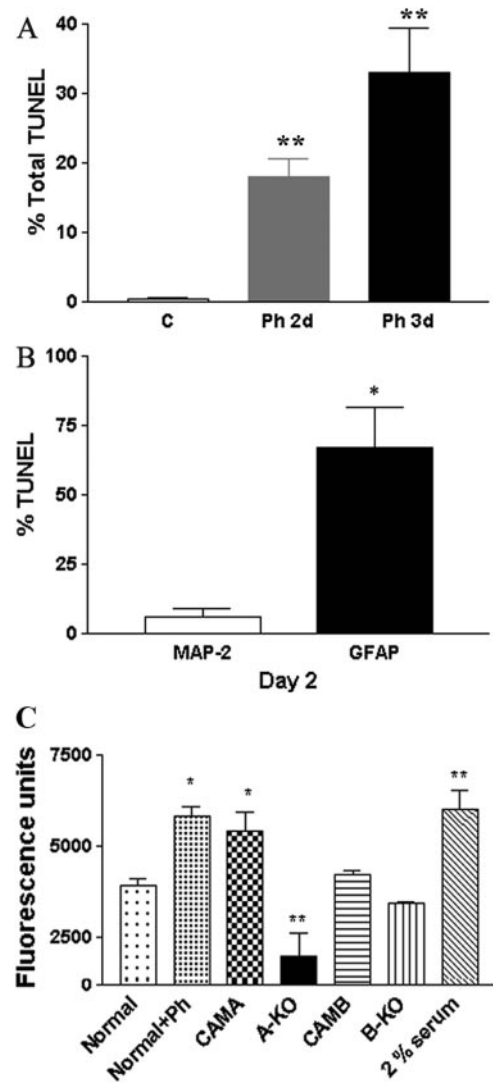
Fig. 8. α_1-ARs regulate apoptosis and migration of neonatal progenitors. A, normal neonatal neurospheres treated with 10 μM phenylephrine for 0 (control), 2, or 3 days increase the number of TUNEL-positive cells. B, TUNEL-positive cells expressed GFAP but not MAP2. C, dissociated normal neonatal neurospheres treated with 10 μM phenylephrine or CAM α_{1A}-AR-derived neurospheres increased migration comparable with 2% serum. α_{1A}-AR KO-derived neurospheres displayed decreased migration. Total cells counted ranged from 40 to 240 per coverslip using at least three different cell preparations tested. *, $P < 0.05$; **, $P < 0.01$.

ulated both early (Dlx2, Mash1) and late stage (NeuroD) homeobox and bHLH mRNA in neonatal neurospheres, suggesting their regulation of neuronal maturation (Fig. 6).

However, in adult mice, α_1-ARs seemed to regulate gliogenesis. Isolated adult neurospheres increased markers for CC1- and GFAP-positive glia upon α_1-AR stimulation while down-regulating NMDA receptor levels, which are located predominantly on neurons (Köhr, 2006) (Fig. 9). In vivo, S100-positive glial and βIII tubulin-positive progenitors colocalized with α_1-ARs in the olfactory bulb, whereas α_1-AR cells in the SVZ were negative for either marker. In previous reports, we found that α_1-AR subtypes were present in NG2-positive oligodendrocytes and were weakly expressed in CC1-positive mature oligodendrocytes in adult mice (Papay et al., 2004, 2006).
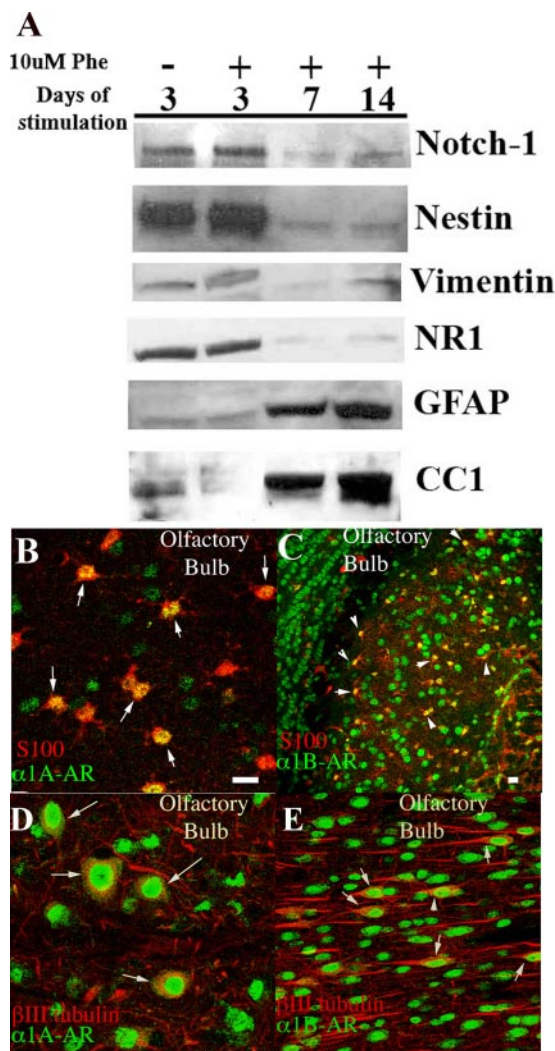
Fig. 9. α_1-ARs differentiate normal adult neurospheres into glial cells. A, Western blot analysis of normal adult neurospheres stimulated with phenylephrine (Phe 10 μM) decreased the expression of markers associated with undifferentiated stem cells, such as notch-1, nestin, and vimentin, but increased the expression of GFAP and CC1, markers for astrocytes and oligodendrocytes, respectively. The NMDA receptor neuronal marker NR1 decreased in expression upon α_1-AR stimulation. Similar results repeated in another normal adult neurosphere cell line. Both adult neurosphere cell lines were negative for the neuronal markers tyrosine hydroxylase, GAD-65/67, and dopamine β-hydroxylase. α_{1A}-AR promoter-EGFP (B and D) or α_{1B}-AR-EGFP tagged (C and E) cells (green) colocalized (arrows) with S100-positive or βIII tubulin-positive cells in the adult olfactory. Mice were aged 2 to 3 months. White bar, 10 μm.

α_{1A}-ARs are likely to also regulate the proliferation of adult neural stem and/or TAP cells. Upon long-term exposure to BrdU and several days of chase, α_{1A}-AR stimulation increased the number of BrdU$^+$ cells in adult SVZ, which was not diluted upon increasing chase (Fig. 5). Because NSCs slowly divide (Morshead et al., 1994), incorporated BrdU would not be lost with increased chase in this cell type. Upon short-term BrdU incorporation, which would label rapidly dividing progenitors (Morshead et al., 1994), α_{1A}-AR stimulation increased BrdU incorporation in the SVZ and SGZ (Fig. 4, A and B). The unexpected high incorporation of BrdU in the SGZ in the α_{1A}-AR KO could be due to spontaneous seizures reported in these mice (Knudson et al., 2007). Seizure activity has been reported to increase neurogenesis in the SGZ (Parent et al., 1997). These data suggest that α_{1A}-ARs are expressed in and regulate the proliferation of both NSCs and progenitors. Further studies are needed to determine whether α_1-ARs also affect the maturation rate of progenitors.

In contrast, α_{1B}-ARs were expressed in the adult RMS in vivo but not in the SVZ (Fig. 2I), and regulated late neuronal maturation factors (Ngn1, Math1) in neonatal neurospheres (Fig. 6). Furthermore, α_{1B}-AR expression was increased in normal neonatal neurospheres undergoing differentiation by phenylephrine (Fig. 3B) or by 1% serum (Fig. 6). Because we do not see a decrease in α_{1A}-AR RNA upon serum-induced differentiation (Fig. 6), our results suggest that the α_{1B}-AR is being induced to increase expression instead of the α_{1A}-AR becoming down-regulated. Overall, these data suggest that the role of the α_{1B}-AR is more important in the later maturation stages of neurogenesis.

Our work suggests that the mechanism of α_{1A}-AR-induced neonatal neurogenesis is due to an initial expansion of NSC/TAP and progenitor cells (Fig. 4A) followed by increased transcription of proneural factors (Fig. 6) and ultimately to the PI3K-dependent survival and maturation of catecholaminergic neurons and GABAergic interneurons (Figs. 7 and 8). The role of PI3K in neonatal neuronal differentiation suggests that α_1-ARs increase prosurvival signals. PI3K has been shown to increase proliferation of adult hippocampal progenitors (Peltier et al., 2007) and induce neuronal differentiation in cell lines (Sánchez et al., 2004). In addition to prosurvival signals, the PI3K/Akt pathway enhances the assembly and activity of bHLH complexes that promote neuronal differentiation (Vojtek et al., 2003). The coordinated increases in the activity of Mash1 and Ngns that are regulated by α_1-ARs (Fig. 6) have been shown to transition neurogenesis from proliferation to neuronal differentiation (Ross et al., 2003). Interestingly, each α_1-AR subtype regulates its own distinct set of proneural transcription factors. Mash1 regulates Dlx2's temporal expression (Poitras et al., 2007), and both genes are regulated by the α_{1A}-AR.

The α_{1A}-AR has been previously confirmed to functionally regulate interneurons (Hillman et al., 2007) and now is confirmed in our work to be involved in their differentiation in the neonate. The decreased expression of $\beta1$ integrin by α_1-AR stimulation is also consistent with differentiation because $\beta1$-integrins have been shown to maintain NSC function (Campos et al., 2004).

The mechanism of α_1-AR regulation of adult gliogenesis remains to be determined. Although α_1-ARs are localized to neurons, progenitors, and glia, we cannot rule out that α_1-AR

regulation of the cerebral microvasculature system does not contribute to neurogenesis or gliogenesis. α_1-ARs regulate the secretion of growth factors and extracellular matrix from endothelium that may affect the NSC niche (Ramírez-Castillejo et al., 2006).

A neuron-to-glia switch occurs naturally in neuroepithelial precursor cells. Early in development, NEPs generate all types of neurons and glia. At later stages, neuroepithelial precursor potential becomes restricted to glia (Kessaris et al., 2008). All of the factors that drive this neuron-glial switch are not known. However, down-regulation of bHLH transcription factors is an important step, driving stem cell transition from a neurogenic toward a gliogenic potential. A microarray study of gene expression changes in the brain of the CAM α_{1B}-AR mice revealed several cell fate genes being regulated that direct both glial (BMP2 receptor, insulin-like growth factor receptor, thyroid hormone and Eph receptors) and neuronal development (brain-derived neurotrophic factor, prolactin) (Yun et al., 2003). It is possible that differential regulation of bHLH transcription factors from neonatal to adult by α_1-ARs accounts for the neuron-glial transition.

Our studies highlight the ability of α_1-ARs to regulate neurogenesis and gliogenesis and offers new treatment options for cell loss due to neurodegeneration. Because proliferation in adult rodents decreases with age (Kuhn et al., 1996), any agent that can increase the proliferation of NSCs and direct differentiation in the adult may be a valuable strategy.

However, long-term activation of the α_{1B}-AR would probably be detrimental as a therapy because CAM α_{1B}-AR mice have an age-progressive neurodegeneration that manifests at 7 to 12 months of age (Zuscik et al., 2000), confirmed in KO mice (Pizzanelli et al., 2009), which may be due to long-term glutamate (Marek and Aghajanian, 1999) or dopamine excitation (Villégier et al., 2003). α_{1A}-AR activation cojoined with specific α_{1B}-AR antagonism may be a preferred treatment option because α_{1B}-AR blockage protects against α-synuclein aggregates and neurotoxicity (Papay et al., 2002). In addition to regulating neurogenesis, the α_{1A}-AR is neuroprotective against seizures and protects interneurons against age-related death (Knudson et al., 2007). Long-term α_{1A}-AR stimulation is also cardioprotective (Huang et al., 2007), which would be an additional benefit of such a class of drugs.

References

Campos LS, Leone DP, Relvas JB, Brakebusch C, Fässler R, Suter U, and ffrench-Constant C (2004) Beta1 integrins activate a MAPK signalling pathway in neural stem cells that contributes to their maintenance. *Development* **131:**3433–3444.

Chen L, Hodges RR, Funaki C, Zoukhri D, Gaivin RJ, Perez DM, and Dartt DA (2006) Effects of alpha1D-adrenergic receptors on shedding of biologically active EGF in freshly isolated lacrimal gland epithelial cells. *Am J Physiol Cell Physiol* **291:**C946–C956.

Gonzalez-Cabrera PJ, Gaivin RJ, Yun J, Ross SA, Papay RS, McCune DF, Rorabaugh BR, and Perez DM (2003) Genetic profiling of α_1-adrenergic receptor subtypes by oligonucleotide microarrays: coupling to interleukin-6 secretion but differences in STAT 3 phosphorylation and gp-130. *Mol Pharmacol* **63:**1104–1116.

Hillman KL, Doze VA, and Porter JE (2007) α_{1A}-Adrenergic receptors are functionally expressed by a subpopulation of cornu ammonis 1 interneurons in rat hippocampus. *J Pharmacol Exp Ther* **321:**1062–1068.

Huang Y, Wright CD, Merkwan CL, Baye NL, Liang Q, Simpson PC, and O'Connell TD (2007) An α_{1A}-adrenergic-extracellular signal-regulated kinase survival signaling pathway in cardiac myocytes. *Circulation* **115:**763–772.

Hwa J, Gaivin R, Porter JE, and Perez DM (1997) Synergism of constitutive activity in α_1-adrenergic receptor activation. *Biochemistry* **36:**633–639.

Jensen BC, Swigart PM, and Simpson PC (2009) Ten commercial antibodies for α_1-adrenergic receptor subtypes are nonspecific. *Naunyn Schmiedebergs Arch Pharmacol* **379:**409–412.

Jin K, Zhu Y, Sun Y, Mao XO, Xie L, and Greenberg DA (2002) Vascular endothelial growth factor (VEGF) stimulates neurogenesis in vitro and in vivo. *Proc Natl Acad Sci U S A* **99:**11946–11950.

Kessaris N, Pringle N, and Richardson WD (2008) Specification of CNS glia from neural stem cells in the embryonic neuroepithelium. *Philos Trans R Soc Lond B Biol Sci* **363:**71–85.

Knudson CA, Carr PA, Perez DM, and Doze VA (2007) α_{1A} Adrenergic receptor overexpression protects hippocampal interneurons (Abstract). *FASEB J* **21:**A1209, 896.6.

Köhr G (2006) NMDA receptor function: subunit composition versus spatial distribution. *Cell Tissue Res* **326:**439–446.

Kuhn HG, Dickinson-Anson H, and Gage FH (1996) Neurogenesis in the dentate gyrus of the adult rat: age-related decrease of neuronal progenitor proliferation. *J Neurosci* **16:**2027–2033.

Lie DC, Song H, Colamarino SA, Ming GL, and Gage FH (2004) Neurogenesis in the adult brain: new strategies for central nervous system diseases. *Annu Rev Pharmacol Toxicol* **44:**399–421.

Lindvall M and Owman C (1981) Autonomic nerves in the mammalian choroid plexus and their influence on the formation of cerebrospinal fluid. *J Cereb Blood Flow Metab* **1:**245–266.

Livak KJ and Schmittgen TD (2001) Analysis of relative gene expression data using real-time quantitative PCR and the 2($-$delta delta C(T)) method. *Methods* **25:**402–408.

Maharaj AS, Saint-Geniez M, Maldonado AE, and D'Amore PA (2006) Vascular endothelial growth factor localization in the adult. *Am J Pathol* **168:**639–648.

Marek GJ and Aghajanian GK (1999) 5-HT2A receptor or α_1-adrenoceptor activation induces excitatory postsynaptic currents in layer V pyramidal cells of the medial prefrontal cortex. *Eur J Pharmacol* **367:**197–206.

Morshead CM, Reynolds BA, Craig CG, McBurney MW, Staines WA, Morassutti D, Weiss S, and van der Kooy D (1994) Neural stem cells in the adult mammalian forebrain: a relatively quiescent subpopulation of subependymal cells. *Neuron* **13:**1071–1082.

Morshead CM and van der Kooy D (2004) Disguising adult neural stem cells. *Curr Opin Neurobiol* **14:**125–131.

O'Connell TD, Rokosh DG, and Simpson PC (2001) Cloning and characterization of the mouse $\alpha_{1C/A}$-adrenergic receptor gene and analysis of an α_{1C} promoter in cardiac myocytes: role of an MCAT element that binds transcriptional enhancer factor-1 (TEF-1). *Mol Pharmacol* **59:**1225–1234.

Pabbathi VK, Brennan H, Muxworthy A, Gill L, Holmes FE, Vignes M, and Haynes LW (1997) Catecholaminergic regulation of proliferation and survival in rat forebrain paraventricular germinal cells. *Brain Res* **760:**22–33.

Papay R, Gaivin R, Jha A, McCune DF, McGrath JC, Rodrigo MC, Simpson PC, Doze VA, and Perez DM (2006) Localization of the mouse alpha1A-adrenergic receptor (AR) in the brain: alpha1AAR is expressed in neurons, GABAergic interneurons, and NG2 oligodendrocyte progenitors. *J Comp Neurol* **497:**209–222.

Papay R, Gaivin R, McCune DF, Rorabaugh BR, Macklin WB, McGrath JC, and Perez DM (2004) Mouse α_{1b}-adrenergic receptor is expressed in neurons and NG2 oligodendrocytes. *J Comp Neurol* **478:**1–10.

Papay R, Zuscik MJ, Ross SA, Yun J, McCune DF, Gonzalez-Cabrera P, Gaivin R, Drazba J, and Perez DM (2002) Mice expressing the α_{1B}-adrenergic receptor induces a synucleinopathy with excessive tyrosine nitration but decreased phosphorylation. *J Neurochem* **83:**623–634.

Parent JM, Yu TW, Leibowitz RT, Geschwind DH, Sloviter RS, and Lowenstein DH (1997) Dentate granule cell neurogenesis is increased by seizures and contributes to aberrant network reorganization in the adult rat hippocampus. *J Neurosci* **17:**3727–3738.

Peltier J, O'Neill A, and Schaffer DV (2007) PI3K/Akt and CREB regulate adult neural hippocampal progenitor proliferation and differentiation. *Dev Neurobiol* **67:**1348–1361.

Pizzanelli C, Lazzeri G, Fulceri F, Giorgi FS, Pasquali L, Cifelli G, Murri L, and Fornai F (2009) Lack of α_{1b}-adrenergic receptor protects against epileptic seizures. *Epilepsia* **50:**59–64.

Poitras L, Ghanem N, Hatch G, and Ekker M (2007) The proneural determinant MASH1 regulates forebrain Dlx1/2 expression through the I12b intergenic enhancer. *Development* **134:**1755–1765.

Ramírez-Castillejo C, Sánchez-Sánchez F, Andreu-Agulló C, Ferrón SR, Aroca-Aguilar JD, Sánchez P, Mira H, Escribano J, and Fariñas I (2006) Pigment epithelium-derived factor is a niche signal for neural stem cell renewal. *Nat Neurosci* **9:**331–339.

Ross SE, Greenberg ME, and Stiles CD (2003) Basic helix-loop-helix factors in cortical development. *Neuron* **39:**13–25.

Sánchez S, Jiménez C, Carrera AC, Diaz-Nido J, Avila J, and Wandosell F (2004) A cAMP-activated pathway, including PKA and PI3K, regulates neuronal differentiation. *Neurochem Int* **44:**231–242.

Santarelli L, Saxe M, Gross C, Surget A, Battaglia F, Dulawa S, Weisstaub N, Lee J, Duman R, Arancio O, et al. (2003) Requirement of hippocampal neurogenesis for the behavioral effects of antidepressants. *Science* **301:**805–809.

Sirviö J and MacDonald E (1999) Central α_1-adrenoceptors: their role in the modulation of attention and memory formation. *Pharmacol Ther* **83:**49–65.

Sun L, Vitolo M, and Passaniti A (2001) Runt-related gene 2 in endothelial cells: inducible expression and specific regulation of cell migration and invasion. *Cancer Res* **61:**4994–5001.

Suslov ON, Kukekov VG, Ignatova TN, and Steindler DA (2002) Neural stem cell heterogeneity demonstrated by molecular phenotyping of clonal neurospheres. *Proc Natl Acad Sci U S A* **99:**14506–14511.

Villégier AS, Drouin C, Bizot JC, Marien M, Glowinski J, Colpaërt F, and Tassin JP (2003) Stimulation of postsynaptic α_{1b}- and α_2-adrenergic receptors amplifies dopamine-mediated locomotor activity in both rats and mice. *Synapse* **50:**277–284.

Vojtek AB, Taylor J, DeRuiter SL, Yu JY, Figueroa C, Kwok RP, and Turner DL (2003) Akt regulates basic helix-loop-helix transcription factor-coactivator complex formation and activity during neuronal differentiation. *Mol Cell Biol* **23:**4417–4427.

Yun J, Gaivin RJ, McCune DF, Boongird A, Papay RS, Ying Z, Gonzalez-Cabrera PJ,

Najm I, and Perez DM (2003) Gene expression profiles of neurodegeneration induced by the α_{1b}-adrenergic receptor: NMDA/GABA$_A$ dysregulation and apoptosis. *Brain* **126:**2667–2681.

Zuscik MJ, Porter JE, Gaivin R, and Perez DM (1998) Identification of a conserved switch residue responsible for selective constitutive activation of the β_2-adrenergic receptor. *J Biol Chem* **273:**3401–3407.

Zuscik MJ, Piascik MT, and Perez DM (1999) Cloning, cell-type specificity and regulatory function of the murine α_{1b}-adrenergic receptor promoter. *Mol Pharmacol* **56:**1288–1297.

Zuscik MJ, Sands S, Ross SA, Waugh DJ, Gaivin RJ, Morilak D, and Perez DM (2000) Overexpression of the α_{1b}-adrenergic receptor causes apoptotic neurodegeneration: a multiple system atrophy. *Nat Med* **6:**1388–1394.

Address correspondence to: Dr. Dianne M. Perez, NB50, 9500 Euclid Avenue, The Cleveland Clinic Foundation, Cleveland, OH 44195. E-mail: perezd@ccf.org